Normal state above the upper critical field in $Fe_{1+y}Te_{1-x}(Se,S)_{x}$

Aifeng Wang (□□□), Erik Kampert, H. Saadaoui, H. Luetkens, Rongwei Hu (□□□), E. Morenzoni, J. Wosnitza, and C. Petrovic

Phys. Rev. B **95**, 184504 — Published 3 May 2017

DOI: 10.1103/PhysRevB.95.184504

Normal state above the upper critical field in $Fe_{1+y}Te_{1-x}(Se,S)_x$

Aifeng Wang (王爱峰),[1] Erik Kampert,[2] H. Saadaoui,[3] H. Luetkens,[3]
Rongwei Hu (胡荣伟),[1,*] E. Morenzoni,[3] J. Wosnitza,[2,4] and C. Petrovic[1]
[1] *Condensed Matter Physics and Materials Science Department, Brookhaven National Laboratory, Upton, New York 11973, USA*
[2] *Hochfeld-Magnetlabor Dresden (HLD-EMFL), Helmholtz-Zentrum Dresden-Rossendorf, D-01314 Dresden, Germany*
[3] *Laboratory for Muon Spin Spectroscopy, Paul Scherrer Institute, CH-5232 Villigen PSI, Switzerland*
[4] *Institut für Festkörperphysik, TU Dresden, D-01062, Dresden, Germany*
(Dated: March 31, 2017)

We have investigated the magnetotransport above the upper critical field (H_{c2}) in $Fe_{1.14}Te_{0.7}Se_{0.3}$, $Fe_{1.02}Te_{0.61}Se_{0.39}$, $Fe_{1.05}Te_{0.89}Se_{0.11}$, and $Fe_{1.06}Te_{0.86}S_{0.14}$. The μSR measurements confirm electronic phase separation in $Fe_{1.06}Te_{0.86}S_{0.14}$, similar to $Fe_{1+y}Te_{1-x}Se_x$. Superconductivity is suppressed in high magnetic fields above 60 T, allowing to gain insight into the normal-state properties below the zero-field superconducting transition temperature (T_c). We show that the resistivity of $Fe_{1.14}Te_{0.7}Se_{0.3}$ and $Fe_{1.02}Te_{0.61}Se_{0.39}$ above H_{c2} is metallic as $T \rightarrow 0$, just like the normal-state resistivity above T_c. On the other hand, the normal-state resistivity in $Fe_{1.05}Te_{0.89}Se_{0.11}$ and $Fe_{1.06}Te_{0.86}S_{0.14}$ is nonmetallic down to lowest temperatures, reflecting the superconductor-insulator (SIT) transition due to electronic phase separation.

PACS numbers: 74.81.-g, 74.25.F-, 74.70.Xa

I. INTRODUCTION

It is important to understand the normal state of iron based superconductors since the mechanism of conductivity carries the information about the interactions and correlations in the electronic system out of which superconductivity develops.[1–4] The conductivity, however, is often connected with crystal lattice imperfections or defects. Granular Al-Ge films host superconducting Al islands embedded in an amorphous Ge matrix.[5,6] In underdoped copper oxides such chemical (crystallographic) phase separation on two space groups is absent; yet the inhomogeneous hole concentration induces nanoscale phase separation into superconducting domains and electronically distinct background.[7] Both granular aluminum and underdoped copper oxides feature metallic state above zero-field T_c. Magnetic-field induced breakdown of superconductivity is expected to give rise to a metallic state below the zero-field T_c in a conventional superconductor. However upon applying pulsed magnetic fields, SIT was reported in both granular aluminum and underdoped copper oxides such as $La_{2-x}Sr_xCuO_4$, $Bi_2Sr_{2-x}La_xCuO_6$, and $Pr_{2-x}Ce_xCuO_{6+\delta}$.[6,8–10] The mechanism of the SIT can stem not only from the Coulomb interaction enhanced by disorder within the BCS framework but also from granularity.[11–13] In granular superconductors, which feature isolated superconducting grains, Josephson tunnelling between the grains establishes the macroscopic superconducting state.

The Fe-based superconductors share many similarities with copper-oxide superconductors, such as the layered crystal structure and superconductivity that emerges by the suppression of an antiferromagnetic ground state.[14,15] Although still quite scarce due to the high upper critical fields, studies of the normal-state electronic transport in FeAs-based superconductors below zero-field T_c have revealed log-T nonmetallic resistivity that is unrelated to SIT.[16] Such studies are also infrequent for FeSe-based superconductors. Yet due to complexity of nanoscale inhomogeneity iron-selenide materials offer an opportunity to correlate conducting states below zero-field T_c in high magnetic fields with the aspects of crystal structure. $K_xFe_{2-y}Se_2$ superconductors feature crystal structure that is phase-separated in two space groups where electronic phase separation comes naturally in superconducting islands immersed in an insulating matrix, just like in granular aluminum.[17–21] On the other hand and similar to copper oxides, $Fe_{1+y}Te_{1-x}Se_x$ superconductors exhibit electronic phase separation below zero-field T_c whereas their crystal structure is chemically inhomogeneous but not phase separated since they crystallize in one space group with defects and interstitial atoms irrespective of Se/Te ratio.[22–31] Whereas SIT has been reported in doped $K_xFe_{2-y}Se_2$,[32,33] the nature of conducting states below zero-field T_c for $H > H_{c2}$ is still unknown in $Fe_{1+y}Te(Se,S)$.

The normal-state resistivity reflects the electronic structure underlying the high-temperature superconductivity and hints at the origin of its mechanism.[34] It is of interest to understand the normal state of FeCh (Ch = S, Se, or Te) in high magnetic fields since $FeCh_4$ tetrahedra constitute potential building-blocks of high-temperature superconductivity. Bulk β-FeSe superconducts below 8.5 K.[35] This can be enhanced up to 15 K by Te doping in bulk $Fe_{1+y}Te_{1-x}Se_x$ or up to about 30 K by pressure or in $K_xFe_{2-y}Se_2$.[28,36,37] FeSe films on $SrTiO_3$ have shown T_c as high as 100 K.[38]

The doping-phase diagrams of $Fe_{1+y}Te_{1-x}Se_x$ and $Fe_{1+y}Te_{1-x}S_x$ indicate a superconducting dome as a function of Se or S doping on Te site.[22,23] They also suggest an electronic phase separation below zero-field T_c in superconducting and magnetic volume fractions.

This allows for investigation of SIT in FeSe superconductors with no crystallographic phase separation inherent to $K_xFe_{2-y}Se_2$.

In this work we have examined normal state in high magnetic fields when superconductivity is suppressed for $x = 0.14$ sulfur and $x = 0.11, 0.30, 0.39$ of Se substitution. We compare the normal-state transport below zero-field T_c in high magnetic fields for materials with different normal-state transport above T_c (metallic vs. nonmetallic) and with different amount of interstitial Fe which favors Kondo-type scattering. These crystals exhibit a different electronic phase separation below zero-field T_c. The volume fractions of superconductivity are about 1% for $x = 0.11$ Se, about 10 % for $x = 0.30$ and $x = 0.39$ Se.[22] We show electronic phase separation below zero-field T_c in $Fe_{1.06}Te_{0.86}S_{0.14}$, similar to $Fe_{1+y}Te_{1-x}Se_x$.[22] We also show that the normal state in $Fe_{1.05}Te_{0.89}Se_{0.11}$ and $Fe_{1.06}Te_{0.86}S_{0.14}$ below zero-field T_c above H_{c2} is nonmetallic whereas the in-plane resistivity below T_c for $Fe_{1.14}Te_{0.7}Se_{0.3}$ and $Fe_{1.02}Te_{0.61}Se_{0.39}$ is metallic for $H > H_{c2}$, just like the the normal state resistivity above the T_c. In the absence of Kondo-type scattering[39,40] which is suppressed in high magnetic fields, the results for $Fe_{1.05}Te_{0.89}Se_{0.11}$ and $Fe_{1.06}Te_{0.86}S_{0.14}$ show clear SIT behavior.[12,13] This is the first observation of SIT in electronically granular Fe superconductors in the absence of crystallographic phase separation, similar to copper oxides.

II. EXPERIMENT

The single crystals used in this study were grown and characterized as described previously.[23,41] Pulsed-field experiments were performed up to 61 T using a magnet with 150 ms pulse duration at the Dresden High Magnetic Field Laboratory. The magnetic field is applied parallel to the c axis to most effectively suppress superconductivity. Data were obtained via a fast data-acquisition system operating with ac current in the kHz range. The exposure of the samples to ambient conditions was minimized by handling the samples in a glove box. The contacts were made on freshly cleaved surfaces inside the glove box using silver paint and platinum wires. The elemental and micro structure analysis were performed using energy-dispersive X-ray spectroscopy in an JEOL JSM-6500 scanning electron microscope.[23,41] The average stoichiometry was determined by examination of multiple points on the crystals. The measured compositions were $Fe_{1.14(2)}Te_{0.70(2)}Se_{0.30(2)}$, $Fe_{1.02(3)}Te_{0.61(4)}Se_{0.39(4)}$, $Fe_{1.05(3)}Te_{0.89(2)}Se_{0.11(2)}$, and $Fe_{1.06(3)}Te_{0.86(1)}S_{0.14(2)}$. The error bars reflect maximum distance from the average stoichiometry (inhomogeneity). Typical crystal size was about 4x1x0.2 mm. The contact resistance was between 10 and 50 Ohms and the excitation current was 0.3 mA which corresponds to a current density of approximately 10^3 A/m^2, ensuring the absence of resistive heating effects. Transverse-field (TF)- and zero-field (ZF)-μSR experiments were carried out at the Paul Scherrer Institute (Villigen, Switzerland) on $Fe_{1.05}Te_{0.89}Se_{0.11}$ in order to detect and quantify magnetic and superconducting phases. The sample was cooled to the base temperature of 5 K in zero field for the ZF-μSR experiments. The ZF- and TF-μSR data were analyzed by using the MUSRFIT software package.[42]

III. RESULTS AND DISCUSSION

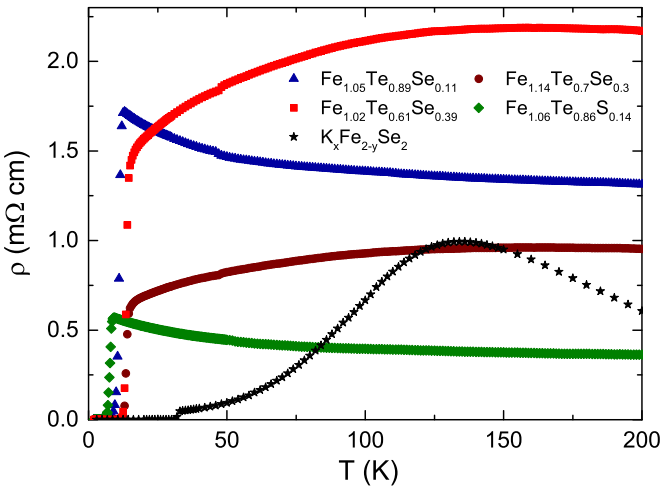

FIG. 1. (a) Temperature dependence of the in-plane resistivity for $Fe_{1.02}Te_{0.61}Se_{0.39}$, $Fe_{1.14}Te_{0.7}Se_{0.3}$, $Fe_{1.05}Te_{0.89}Se_{0.11}$, and $Fe_{1.06}Te_{0.86}S_{0.14}$ single crystals. For comparison we also plot resistivity of $K_xFe_{2-y}Se_2$.

The normal-state resistivities of $Fe_{1.02}Te_{0.61}Se_{0.39}$ and $Fe_{1.14}Te_{0.7}Se_{0.3}$ are metallic, whereas $Fe_{1.05}Te_{0.89}Se_{0.11}$ and $Fe_{1.06}Te_{0.86}S_{0.14}$ feature a temperature dependence of an incoherent metal (Fig. 1).[23,39,43] The resistivity values are higher than of $K_xFe_{2-y}Se_2$ where grain boundaries also contribute due to crystallographic phase separation.[44] We note that the mean free path of $Fe_{1.14}Te_{0.91}S_{0.09}$ is $l = 1.35$ nm.[39] Assuming similar mean free path for $Fe_{1.06}Te_{0.86}S_{0.14}$ investigated here and noting that for $Fe_{1+y}Te_{0.5}Se_{0.5}$ carrier concentration is about $2{\cdot}10^{21}$ cm^{-3},[45] we see that for resistivities of about (1-2) mΩcm, Drude mean free path $l{=}\hbar(3\pi^2)^{1/3}/(e^2\rho_0 n^{2/3})$ should be about (0.3-0.5) nm. This is comparable to interatomic spacing where resistivity should saturate.[46,47] Therefore high temperature resistivity (Fig. 1) should also be affected by the Mott-Ioffe-Regel saturation similar to $SrFe_{2-x}M_xAs_2$ (M=Co,Ni), in addition to localization and inchoherence due to Kondo scattering.[23,39,40,43,48]

The magnetoresistances (MR) at different temperatures for $Fe_{1.14}Te_{0.7}Se_{0.3}$ and $Fe_{1.02}Te_{0.61}Se_{0.39}$ are shown in Figs. 2(a) and 2(b). Superconductivity is suppressed by increasing magnetic field at fixed temperature,

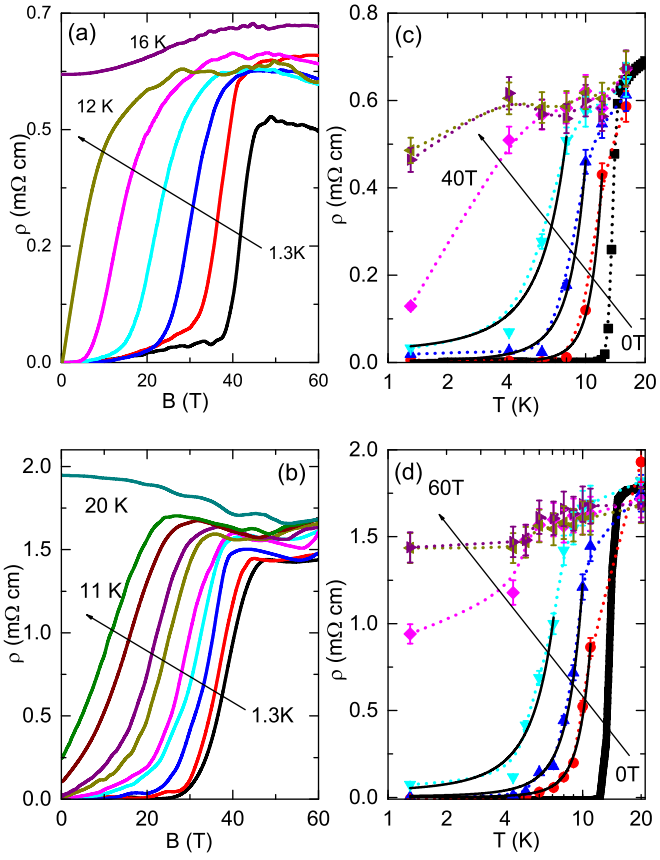

FIG. 2. Magnetic-field dependence of the in-plane resistivity at fixed temperatures for (a) $Fe_{1.14}Te_{0.7}Se_{0.3}$ and (b) $Fe_{1.02}Te_{0.61}Se_{0.39}$. The arrows indicate the direction of increasing temperature. (a) For $Fe_{1.14}Te_{0.7}Se_{0.3}$, data were collected at 1.3, 4.0, 6.0, 8.0, 10.0, 12.1, and 16.0 K. (b) For $Fe_{1.02}Te_{0.61}Se_{0.39}$, data were collected at 1.3, 4.4, 5.1, 6.0, 7.1, 8.0, 9.0, 10.0, 11.0, and 20.0 K. Temperature dependence of the in-plane resistivity for (c) $Fe_{1.14}Te_{0.7}Se_{0.3}$ and (d) $Fe_{1.02}Te_{0.61}Se_{0.39}$. The data were obtained from fixed-temperature pulsed magnetic-field sweeps. The arrows indicate the direction of increasing magnetic field: 0, 10, 20, 30, 40, 50, and 60 T. Note that 50 and 60 Tesla data nearly overlap with each other in both (c) and (d).

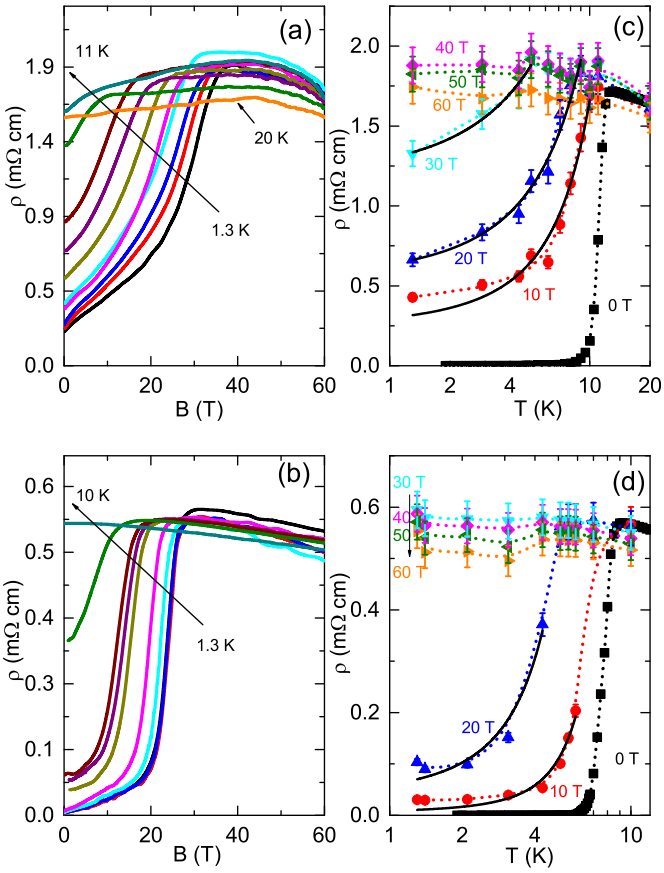

FIG. 3. Magnetic-field dependence of the in-plane resistivity vs magnetic field for (a) $Fe_{1.05}Te_{0.89}Se_{0.11}$ and (b) $Fe_{1.06}Te_{0.86}S_{0.14}$. Temperature dependence of the in-plane resistivity for (c) $Fe_{1.05}Te_{0.89}Se_{0.11}$ and (d) $Fe_{1.06}Te_{0.86}S_{0.14}$. The data were obtained from the results shown in panels (a,b). The arrows indicate the direction of increasing magnetic field: 0, 10, 20, 30, 40, 50, and 60 T.

and the transition in field-dependent ρ_{ab} data is shifted to lower magnetic fields with increasing temperature. We observe a finite resistance in the superconducting state of $Fe_{1.14}Te_{0.7}Se_{0.3}$, which may be caused either by experimental artifacts or by thermally activated vortex-flux motion. The upper critical fields of $Fe_{1.14}Te_{0.7}Se_{0.3}$ and $Fe_{1.02}Te_{0.61}Se_{0.39}$ are about 45 T, consistent with previous reports.[41,49] The temperature dependence of the resistivity of $Fe_{1.14}Te_{0.7}Se_{0.3}$ and $Fe_{1.02}Te_{0.61}Se_{0.39}$ is presented in Figs. 2(c) and 2(d). The normal-state resistivity of $Fe_{1.14}Te_{0.7}Se_{0.3}$ continues to decrease below T_c and is nearly constant between 4 and 12 K. A similar behavior was observed in $Fe_{1.02}Te_{0.61}Se_{0.39}$ and FeSe, where the high-field resistivity at T $\leq$ 1 K is almost temperature independent.[41,50]

Figures 3(a) and 3(b) show how the superconducting transitions of $Fe_{1.05}Te_{0.89}Se_{0.11}$ and $Fe_{1.06}Te_{0.86}S_{0.14}$ shift to low field with increasing temperature. Superconductivity is suppressed at all temperatures below zero-field T_c above 40 T, revealing a nonmetallic normal state resistivity with decreasing temperature [Figs. 3(c) and 3(d)]. We note that resistivity as a function of magnetic field near H_{c2} is non-monotonic (Fig. 3), similar to granular Al and $La_{2-x}Sr_xCuO_4$.[6,13,51] Within the framework of SIT theory in granular electronic systems, this is due to a competition between gap opening in the density of states and enhancement of conductance due to superconducting fluctuations.[13] In disordered InO, ultrathin TiN or granular Al-Ge films the negative MR in high magnetic fields was explained by the destruction of fluctuation-related quasilocalized superconducting pairs.[6,52,53] In an array of superconducting grains in an insulating matrix magnetic field suppress superconductivity in individual grains.[13] Above H_{c2}, virtual Cooper pairs can persist; they reduce density of states (DOS) and cannot travel

between grains, thus suppressing resistivity. This is the correction to Drude resistivity due to DOS reduction. There are also Aslamazov-Larkin (transport channel via fluctuating Cooper pairs) and Maki-Thompson (coherent scattering of electrons forming Cooper pairs on impurities) corrections to Drude resistivity.[54–57] However, at low temperatures and in high magnetic fields $H > H_{c2}$ the DOS reduction is dominant.[13] This leads to a negative MR especially at fields above H_{c2} of individual grains as seen experimentally in granular Al-Ge films.[6]

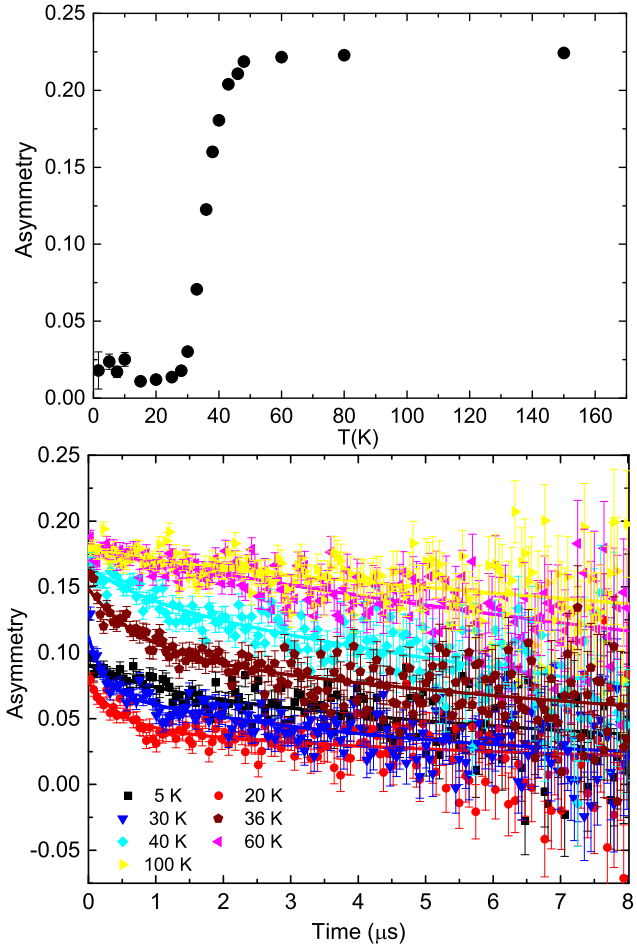

FIG. 4. (a) Amplitude of the precessing asymmetry signal in weak transverse field (5 mT) for $Fe_{1.12}Te_{0.83}S_{0.11}$. The drop of the signal indicates bulk magnetism ($\sim$ 100 % volume fraction) below 37 K. (b) Corresponding zero-field data showing the onset of magnetism below $\sim$ 50 K. Lines are fit to the time evolution of the polarization. See text for details.

In general, it should also be noted that the conductance $g = 1/R$ where R is the sample resistance of an inhomogeneous superconducting crystal such as granular aluminum films or $K_xFe_{2-y}Se_2$ can be approximated as $g = g_{sc} + g_{nsc}$ where g_{sc} and g_{nsc} are contributions from the superconducting and nonsuperconducting parts. In the superconducting state g_{sc} is infinite and g_{nsc} is short-circuited by the superconducting channel. In the normal state the non-superconducting grains may also contribute to electronic transport when their conductivity is not very small when compared to superconducting grains.

In contrast to $K_xFe_{2-y}Se_2$ which features phase separation where metallic grains (I4/mmm space group) are embedded in the insulating/magnetic matrix (I4/m space group),[17–21,32,33,58–61] $Fe_{1+y}Te_{1-x}(Se,S)_x$ crystallize in a single space group without crystallographic phase separation, albeit with the presence of random excess interstitial Fe, inhomogeneous Fe-(Te,Se) bond lengths [i.e., $Fe(Te,Se)_4$ tetrahedra] due to deviations of the local structure from the average and possible defects on Te site.[23,29–31,62] On lowering the temperature magnetism appears before superconductivity appears in $Fe_{1+y}Te_{1-x}(Se,S)_x$; however magnetism coexists with the superconductivity only in the superconducting state below T_c and H_{c2}.[22] In the normal state the two-phase electronic conduction is absent.

In addition to the electrical-transport measurements, we have performed μSR measurements on $Fe_{1.12}Te_{0.83}S_{0.11}$ in order to probe the volume fraction of superconducting and magnetic phases. The $Fe_{1.12}Te_{0.83}S_{0.11}$ has a similar onset T_c as $Fe_{1.06}Te_{0.88}S_{0.14}$ [8.6(1) K vs 8.7(1)], but lower zero-resistance T_c [3.5(1) vs 7.0(1) K] and only a small diamagnetic signal in the magnetic susceptibility indicating percolative superconductivity.[23] Fig. 4(a) shows the temperature dependence of the amplitude of the muon spin precession asymmetry in a weak transverse field. This measurement allows us to determine the magnetic volume fraction of the sample. In a nonmagnetic environment the local field sensed by the muons is determined by the applied field and a weakly damped muon spin precession is observed. If a fraction of the sample becomes magnetic muons stopping in that environment quickly depolarize since the local field is much larger than the applied field and this fraction does not contribute to the precessing amplitude. The observed asymmetry is therefore a measure of the non-magnetic volume fraction of the sample. The drop in asymmetry [Fig. 4(a)] and the fast relaxation at early times in the zero-field polarization spectra [Fig. 4(b)] indicate a bulk magnetic transition at higher temperatures than superconducting T_c. From Fig. 4(a) we determine the transition temperature T_m (defined by the 50% drop in amplitude) to be 37 K with an onset at 50 K. The volume fraction below the transition of the magnetic phase is nearly 100 %. The fact that above 50 K the asymmetry reaches only 0.22 and not 0.26 as it should be in this experimental setup means that there are some magnetic impurities (probably clusters) producing a signal loss at all measured temperatures up to room temperature. A similar effect has been observed in many Fe-based superconductors.[22] Below $\sim$ 15 K, the μSR signal increases reflecting a $\sim$ 10 % non-magnetic fraction below the temperature of T_c onset. This shows that superconductivity while only filamentary or localized competes with magnetism for the sample

volume. We found by μSR studies a similar filamentary superconductivity but with higher T_m (50 K for 50% drop and 70 K onset temperature) and smaller bulk magnetic fraction in $Fe_{1.12(3)}Te_{0.97(1)}S_{0.03(2)}$. Overall the results indicate that, at least in this part of the phase diagram, $Fe_{1+y}Te_{1-x}S_x$ features similar electronic granularity (phase separation) as the Se-substituted compounds below zero-field T_c.[22]

In the superconducting region near the SIT when $H < H_{c2}$, the resistivity of a granular superconductors behaves as $R = R_0 \exp(T/T_0)$ ("inverse Arrhenius law") due to the destruction of quasi-localized Cooper pairs by superconducting fluctuations.[12] The resistivity between 10 T up to about H_{c2} (of 20-40 T) for all investigated crystals is in agreement [solid lines in Figs. 2(b), 2(d), 3(b), and 3(d)] with the bosonic SIT scenario prediction, even in $Fe_{1.14}Te_{0.7}Se_{0.3}$ and $Fe_{1.02}Te_{0.61}Se_{0.39}$ where resistivity saturates above 50 T below about 10 K [Fig. 2(b) and 2(d)].

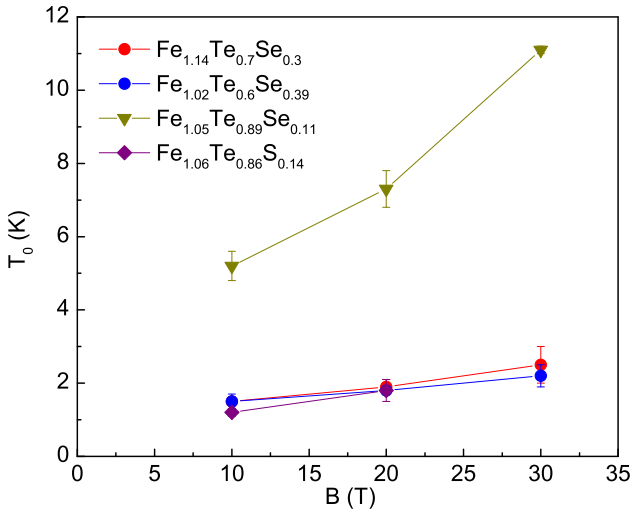

FIG. 5. Values of characteristic temperature T_0 from the $R = R_0 \exp(T/T_0)$ fits for $Fe_{1.14}Te_{0.7}Se_{0.3}$, $Fe_{1.02}Te_{0.61}Se_{0.39}$, $Fe_{1.05}Te_{0.89}Se_{0.11}$, and $Fe_{1.06}Te_{0.86}S_{0.14}$ when resistivity is dominated by superconductivity in the context of SIT.

Fig. 5 shows the values of T_0 from the $R = R_0 \exp(T/T_0)$ fits for $Fe_{1.14}Te_{0.7}Se_{0.3}$ [Fig. 2(c)], $Fe_{1.02}Te_{0.61}Se_{0.39}$ [Fig. 2(d)], $Fe_{1.05}Te_{0.89}Se_{0.11}$ [Fig. 3(c)], and $Fe_{1.06}Te_{0.86}S_{0.14}$ [Fig. 3(d)]. Within the scope of SIT theory the energy scale T_0 is related to the localization length ξ as $T_0 \sim e^2/a\kappa\xi$ where κ is effective dielectric constant and a is the average grain size.[13] As magnetic field is increased between 10 T and 30 T, the value of T_0 increases in all investigated materials. This would correspond to an decrease in localization length, perhaps from coupled clusters of grains to a single grain.[13] The values of T_0 and its increase in magnetic field is higher for $Fe_{1.05}Te_{0.89}Se_{0.11}$ where superconducting volume fraction is minute (about 1%) when compared to other investigated crystals [(10-20) %].

Whereas magnetic domains are separate in space and coexist with superconductivity at the nano- to meso-scale in $K_xFe_{2-y}Se_2$ and some copper oxides,[17,19,63] there is evidence for the two order parameter coexistence on the atomic scale in $Fe_{1+y}Te_{1-x}(Se,S)_x$ below zero-field T_c.[22] Moreover, electronic transport in the normal state above zero-field T_c in $Fe_{1+y}Te_{1-x}(S)_x$ is dominated by the incoherent magnetic Kondo-type scattering that arises due to local moments entanglement with itinerant electrons.[39,40,64,65] The local moments in $Fe_{1+y}Te_{1-x}(Se,S)_x$ stem from the localized iron d orbitals in $FeCh_4$ tetrahedra as well as from the interstitial excess Fe (y).[66] However, it is plausible that pulsed magnetic fields of 60 T would suppress Kondo scattering given that estimated value of Kondo temperature from scattering is about 24 K in $Fe_{1+y}Te_{0.91}S_{0.09}$ or about 60 K in $FeTe_{0.9}Se_{0.1}$.[39,67]

The chalcogen puckering in $FeCh_4$ promotes itinerancy at the expense of localization.[68,69] A high-field non-metallic normal state below T_c has been observed in $Fe_{1.06}Te_{0.86}S_{0.14}$ (Fig. 3) which has less interstitial iron (y) (outside of $FeCh_4$) when compared to $Fe_{1.14}Te_{0.7}Se_{0.3}$ [Fig. 2(c)] that is metallic below T_c. In the absence of Kondo-type scattering, this could suggest less localized Fe-d orbitals in $FeCh_4$ in Fe_{1+y}(Te,Se) than Fe_{1+y}(Te,S). This is consistent with smaller anion height (i.e., smaller $FeCh_4$ puckering) in $Fe_{1+y}Te_{1-x}(S)_x$ when compared to $Fe_{1+y}Te_{1-x}(Se)_x$.[70,71] Therefore the SIT above H_{c2} and below T_c in in $Fe_{1.06}Te_{0.86}S_{0.14}$ is connected with the electronic phase separation.

IV. CONCLUSION

In summary, we have investigated the normal-state resistivity of $Fe_{1.14}Te_{0.7}Se_{0.3}$, $Fe_{1.02}Te_{0.61}Se_{0.39}$, $Fe_{1.05}Te_{0.89}Se_{0.11}$, and $Fe_{1.06}Te_{0.86}S_{0.14}$ below T_c in pulsed magnetic fields. The μSR measurements confirm electronic phase separation in $Fe_{1.06}Te_{0.86}S_{0.14}$, similar to $Fe_{1+y}Te_{1-x}Se_x$. In contrast to $Fe_{1.14}Te_{0.7}Se_{0.3}$ and $Fe_{1.02}Te_{0.61}Se_{0.39}$, the normal-state resistivity in $Fe_{1.05}Te_{0.89}Se_{0.11}$ and $Fe_{1.06}Te_{0.86}S_{0.14}$ shows clear SIT behavior below zero-field T_c in high magnetic fields above H_{c2} and is also nonmonotonic near H_{c2} as expected for SIT in granular electronic systems.[13]

V. ACKNOWLEDGEMENTS

We thank I. Zaliznyak for useful discussions. Work at Brookhaven is supported by the Center for Emergent Superconductivity, an Energy Frontier Research Center funded by the U.S. DOE, Office for Basic Energy Science (HL and CP). We acknowledge the support of HLD at HZDR, member of the European Magnetic Field Laboratory (EMFL). CP acknowledges support by the Alexander von Humboldt Foundation.

* Present address: Department of Physics, University of Maryland, College Park, MD 20742-4111, USA.

[1] Z. P. Yin, K. Haule and G. Kotliar, Nature Materials **10**, 932 (2011).
[2] Pengcheng Dai, Jiangping Hu and E. Dagotto, Nature Physics **8**, 709 (2012).
[3] L. de Medici, G. Giovannetti and M. Capone, Phys. Rev. Lett. **112**, 177001 (2014).
[4] F. Hardy, A. E. Bohmer, D. Aoki, P. Burger, T. Wolf, P. Schweiss, R. Heid, P. Adelmann, Y. X. Yao, G. Kotliar, J. Schmalian, and C. Meingast, Phys. Rev. Lett. **111**, 027002 (2013).
[5] Y. Shapira and G. Deutscher, Phys. Rev. B **27**, 4463 (1983).
[6] A. Gerber, A. Milner, G. Deutscher, M. Karpovsky, and A. Gladkikh, Phys. Rev. Lett. **78**, 4277 (1997).
[7] K. M. Lang, V. Madhavan, J. E. Hoffman, H. Eisaki, S. Uchida and J. C. Davis, Nature (London) **415**, 412 (2002)
[8] G. S. Boebinger, Y. Ando, A. Passner, T. Kimura, M. Okuya, J. Shimoyama, K. Kishio, K. Tamasaku, N. Ichikawa, and S. Uchida, Phys. Rev. Lett. **77**, 5417 (1996).
[9] S. Ono, Y. Ando, T. Murayama, F. F. Balakirev, J. B. Betts, and G. S. Boebinger, Phys. Rev. Lett. **85**, 638 (2000).
[10] P. Fournier, P. Mohanty, E. Maiser, S. Darzen, T. Venkatesan, C. J. Lobb, G. Czjzek, R. A. Webb, and R. L. Greene, Phys. Rev. Lett. **81**, 4720 (1998).
[11] M. Wallin, E. S. Sorensen, S. M. Girvin and A. P. Young, Phys. Rev. B **49**, 12115 (1994).
[12] V. F. Gantmakher, and V. T. Dolgopolov, Phys. Usp. **53**, 1 (2010).
[13] I. S. Beloborodov, A. V. Lopatin, V. M. Vinokur, and K. B. Efetov, Rev. Mod. Phys. **79**, 469 (2007).
[14] J. C. S. Davis and D. H. Lee, Proc. Nat. Ac. Sci. **1**, 1 (2016).
[15] Q. Si and E. Abrahams, Nat. Rev. Mater. **22**, 087410 (2013).
[16] S. C. Riggs, J. B. Kemper, Y. Jo, Z. Stegen, L. Balicas, G. S. Boebinger, F. F. Balakirev, A. Miglion, H. Chen, R. H. Liu, and X. H. Chen, Phys. Rev. B **79**, 212510 (2009).
[17] D. H. Ryan, W. N. Rowan-Weetaluktuk, J. M. Cadogan, R. Hu, W. E. Straszheim, S. L. Budko, and P. C. Canfield, Phys. Rev. B **83**, 104526 (2011).
[18] W. Bao, Q.Z. Huang, G. F. Chen, M. A. Green, D. M. Wang, J. B. He and Y. M. Qiu, Chin. Phys. Lett. **28**, 086104(2011).
[19] W. Li, H. Ding, P. Deng, K. Chang, C. Song, Ke He, L. Wang, X. Ma, J. P. Hu, X. Chen and Q.K. Xue, Nature **8**, 126 (2012).
[20] F. Chen, M. Xu, Q. Q. Ge, Y. Zhang, Z. R. Ye, L. X. Yang, Juan Jiang, B. P. Xie, R. C. Che, M. Zhang, A. F. Wang, X. H. Chen, D.W. Shen, J. P. Hu, and D. L. Feng, Phys. Rev. X **1**, 021020 (2011).
[21] R. H. Yuan, T. Dong, Y. J. Song, P. Zheng, G. F. Chen, J. P. Hu, J. Q. Li, and N. L. Wang, Sci. Rep. **2**, 221 (2012).
[22] R. Khasanov, M. Bendele, A. Amato, P. Babkevich, A. T. Boothroyd, A. Cervellino, K. Conder, S. N. Gvasaliya, H. Keller, H.-H. Klauss, H. Luetkens, V. Pomjakushin, E. Pomjakushina, and B. Roessli, Phys. Rev. B **80**, 140511 (2009).
[23] R. Hu, E. S. Bozin, J. B. Warren, and C. Petrovic, Phys. Rev. B **80**, 214514 (2009).
[24] Xiaobo He, Guorong Li, Jiandi Zhang, A. B. Karki, Rongying Jin, B. C. Sales, A. S. Sefat, M. A. McGuire, D. Mandrus, and E. W. Plummer, Phys. Rev. B **83**, 220502 (2011).
[25] Hefei Hu, Jian-Min Zuo, Jinsheng Wen, Zhijun Xu, Zhiwei Lin, Qiang Li, Genda Gu, Wan Kyu Park, and Laura H Greene, New J. Phys. **13**, 053031 (2011).
[26] Shiliang Li, Clarina de la Cruz, Q. Huang, Y. Chen, J. W. Lynn, Jiangping Hu, Yi-Lin Huang, Fong-Chi Hsu, Kuo-Wei Yeh, Maw-Kuen Wu, and Pengcheng Dai, Phys. Rev. B **79**, 054503 (2009).
[27] Kazumasa Horigane, Haruhiro Hiraka and Kenji Ohoyama, J. Phys. Soc. Jpn. **78**, 074718 (2009).
[28] K.-W. Yeh, T. W. Huang, Y. L. Huang, T. K. Chen, F. C. Hsu, P. M. Wu, Y. C. Lee, Y. Y. Chu, C. L. Chen, J. Y. Luo, D. C. Yan, and M. K. Wu, EPL **84**, 37002 (2008).
[29] A. Iadecola, B. Joseph, A. Puri, L. Simonelli, Y. Mizuguchi, D. Testemale, O. Proux, J.-L. Hazemann, Y. Takano and N. L, Saini, J. Phys. Condens. Matter **23**, 425701 (2011).
[30] D. Louca, K. Horigane, A. Llobet, R. Arita, S. Ji, N. Katayama, S. Konbu, K. Nakamura, T.-Y. Koo, P. Tong, and K.Yamada, Phys. Rev. B **81**, 134524 (2010).
[31] B. Joseph, A. Iadecola, A. Puri, L. Simonelli, Y. Mizuguchi, Y. Takano, and N. L. Saini, Phys. Rev. B **82**, 020502 (2010).
[32] K. F. Wang, H. Ryu, E. Kampert, M. Uhlarz, J. Warren, J. Wosnitza, and C. Petrovic, Phys. Rev. X **4**, 031018 (2014).
[33] H. Ryu, F. Wolff-Fabris, J. B. Warren, M. Uhlarz, J. Wosnitza, and C. Petrovic, Phys. Rev. B **90**, 020502(R) (2014).
[34] P. B. Allen, W. E. Picket and H. Krakauer, Phys. Rev. B **37**, 7482 (1998).
[35] F. C. Hsu, J. Y. Luo, K. W. Yeh, T. K. Chen, T. W. Huang, P. M. Wu, Y. C. Lee, Y. L. Huang, Y. Y. Chu, D. C. Yan, and M. K. Wu, Proc. Natl. Acad. Sci. USA **105**, 14262 (2008).
[36] S. Medvedev, T. M. McQueen, I. A. Troyan, T. Palasyuk, M. I. Eremets, R. J. Cava, S. Naghavi, F. Casper, V. Ksenofontov, G.Wortmann, and C. Felser, Nat. Mater. **8**, 630 (2009).
[37] J. Guo, S. Jin, G. Wang, S. Wang, K. Zhu, T. Zhou, M. He, and X. Chen, Phys. Rev. B **82**, 180520(R) (2010).
[38] J. F. Ge, Z. L. Liu, C. H. Liu, C. L. Gao, D. Qian, Q. K. Xue, Y. Liu, J. F. Jia, Nat. Mater. **14**, 258 (2015).
[39] H. Lei, R. Hu, E. S. Choi, J. B. Warren, and C. Petrovic, Phys. Rev. B **81**, 184522 (2010).
[40] I. A. Zaliznyak, Zhijun Xu, John M. Tranquada, Genda Gu, Alexei M. Tsvelik and Matthew B. Stone Phys. Rev. Lett. **107**, 216403 (2011).
[41] H. Lei, R. Hu, E. S. Choi, J. B. Warren, and C. Petrovic, Phys. Rev. B **81**, 094518 (2010).
[42] A. Suter and B. M. Wojek, Physics Procedia **30**, 69 (2012).
[43] N. Stojilovic, A. Koncz, L. W. Kohlman, R. Hu, C. Petrovic, and S. V. Dordevic, Phys. Rev. B **81**, 174518 (2010).
[44] Hechang Lei and C. Petrovic, Phys. Rev. B **83**, 184504 (2011).
[45] Y. Liu, R. K. Kremer and C. T. Lin, Supercond. Sci. Technol. **24**, 035102 (2011).
[46] O. Gunnarson, M. Calandra and J. E. Han, Rev. Mod. Phys. **75**, 1085 (2003).
[47] N. E. Hussey, K. Takenaka and H. Takagi, Phil. Mag. **84**, 2847 (2004).
[48] P. L. Bach, S. R. Saha, K. Kirshenbaum, J. Paglione and

R. L. Greene, Phys. Rev. B **83**, 212506 (2011).
[49] J. L. Her, Y. Kohama, Y. H. Matsuda, K. Kindo, W.-H. Yang, D. A. Chareev, E. S. Mitrofanova, O. S. Volkova, A N Vasiliev, and J.-Y. Lin, Supercond. Sci. Technol. **28**, 045013 (2015).
[50] S. I. Vedeneev, B. A. Piot, D. K. Maude, and A. V. Sadakov, Phys. Rev. B **87**, 134512 (2013).
[51] Y. Ando, G. S. Boebinger, A. Passner, T. Kimura and K. Kishio, Phys. Rev. Lett. **75**, 4662 (1995).
[52] M. A. Paalanen, A. F. Hebard, and R. R. Ruel, Phys. Rev. Lett. **69**, 1604 (1992).
[53] T. I. Baturina, and C. Strunk, Phys. Rev. Lett. **98**, 127003 (2007).
[54] L. G. Aslamazov and A. I. Larkin, Fiz. Tverd. Tela (Leningrad) **10**, 1104 (1968).
[55] K. Maki Prog. Theor. Phys. **39**, 897 (1968).
[56] K. Maki Prog. Theor. Phys. **40**, 193 (1968).
[57] R. S. Thompson, Phys. Rev. B **1**, 327 (1970).
[58] D. Louca, K. Park, B. Li, J. Neuefeind and J. Yan, Sci. Rep. **3**, 2047 (2013).
[59] Z. Wang, Y. J. Song, H. L. Shi, Z. W. Wang, Z. Chen, H. F. Tian, G. F. Chen, J. G. Guo, H. X. Yang, and J. Q. Li, Phys. Rev. B **83**, 140505 (2011).
[60] X. Ding, D. Fang, Z. Wang, H. Yang, J. Liu, Q. Deng, G. Ma, and C. Meng, Nature Comm. **4**, 1897 (2013).
[61] Z. Wang, Y. Cai, Z. W. Wang, C. Ma, Z. Chen, H. X. Yang, H. F. Tian, and J. Q. Li, Phys. Rev. B **91**, 064513 (2015).
[62] S. Rössler, D. Cherian, S. Harikrishnan, H. L. Bhat, S. Elizabeth, J. A. Mydosh, L. H. Tjeng, F. Steglich, and S. Wirth, Phys. Rev. B **82**, 144523 (2010).
[63] A. T. Savici, Y. Fudamoto, I. M. Gat, T. Ito, M. I. Larkin, Y. J. Uemura, G. M. Luke, K. M. Kojima, Y. S. Lee, M. A. Kastner, R. J. Birgenau, and K. Yamada, Phys. Rev. B **66**, 014524 (2002).
[64] I. A. Zaliznyak, A. T. Savici, M. Lumsden, A. Tsvelik, R. Hu, and C. Petrovic, Proc. Natl. Acad. Sci. US **112**, 10316 (2015).
[65] S. Ducatman, R. M. Fernandes and N. B. Perkins, Phys. Rev. B **90**, 165123 (2014).
[66] A. Subedi, L. Zhang, D. J. Singh and M. H. Du, Phys. Rev. B **78**, 134514 (2008).
[67] Myron B. Salamon, Nicholas Cornell, Marcelo Jaime, Fedor F. Balakirev, Anvar Zakhidov, Jijie Huang and Haiyan Wang, Sci. Rep. **6**, 21469 (2015).
[68] V. Cvetkovic and Z. Tesanovic, Europhys. Lett. **85**, 37002 (2009).
[69] L. Zhang, D. J. Singh and M. H. Du, Phys. Rev. B **79**, 012506 (2009).
[70] H. Okabe, N. Takeshita, K. Horigane, T. Murinaka, and J. Akimitsu, Phys. Rev. B **81**, 205119 (2010).
[71] Y. Mizuguchi,Y. Hara, K. Deguchi,S. Tsuda, T. Yamaguchi,K. Takeda, H. Kotegawa,H. Tou, and Y. Takano, Supercond. Sci. Technol. **23**, 054013 (2010).